Chaos generation with impulse control: Application to Non-Chaotic Systems and Circuit Design

Kun Tian, Celso Grebogi, and Hai-Peng Ren, *Senior Member, IEEE*

***Abstract*—Chaos has been successfully applied in many fields to improve the performance of engineering systems, such as communication, vibration compact, and mixing. Generating chaos from originally non-chaotic systems is a relevant topic because of potential applications. In this work, the impulse control is shown to generate chaos from non-chaotic system. Using non-chaotic Chen system as an example, we prove by analytical and numerical methods that chaos is indeed generated. The features of the chaos generated by impulse control are analysed using Lyapunov exponents, bifurcation diagram, power spectrum, Poincaré mapping and Kaplan-Yorke dimension. Furthermore, we demonstrate the chaotic attractor generation by impulse control using a circuit experiment. The last but not minor point is that the existence of topological horseshoe is given by rigorous computer-aided proof.**

***Index Terms*—Chaos generation; Impulse control; Nonlinear dynamics; Chen Circuit; Topological Horseshoe.**

I. Introduction

As a natural phenomenon, like diverse weather, chaos is an apparently stochastic motion in deterministic nonlinear systems. Chaos has been extensively investigated since Lorenz reported a sensitive dependence on initial condition in a weather prediction model [1], referred by him as the famous butterfly effect. Chaos attracted a lot of attention from the physics community once it was reported, because this phenomenon violates the common cognition about the deterministic and stochastic concepts. On the one hand, random like motion of a system in chaotic state was considered to be harmful in engineering fields. Therefore, lots of efforts were given to eliminate or control chaos in the systems, which led to the seminal work of chaos control in 1990, namely, the OGY control [2]. After the OGY method, time-delay feedback [3], linear feedback [4], [5], impulse control [6], [7], and others, were reported to control chaos.

On the other hand, since NASA reported to have sent a satellite that accomplished its main task to far away cruise mission just by using sensitive dependence of chaos on initial condition, the features of chaos were recognized to be useful in engineering applications. The broad spectrum property of chaotic signals is used for decreasing the noise in power switching converter [8], for improving the randomness of spreading sequence in spread spectrum communications [9], [10], for improving the energy efficiency of vibration compaction [11], [12] and in liquid mixing operations [13]. The ergodicity of chaotic systems is used to improve the searching ability of optimization algorithms [14]–[16]. Additional properties from chaotic dynamics are being used in engineering applications to improve the efficiency and/or performance of practical systems. For example, chaos was reported to be used in commercial fiber-optic link in Europe to improve the transmission rate [17] and chaos was proposed to be used in IEEE standard for local networks [18]. Chaotic signal in communication system was proved to be optimal in the sense of the simplest matched filter used to achieve maximum signal to noise ratio at receivers [19]. Lyapunov invariance property of chaos, after being transmitted through wireless communication channel, can be used to resist inter-symbol interference [20]–[22]. Chaotic shape-forming filter can also be used to encode arbitrary binary bit sequence together with differential chaos shift key configuration so as to improve the bit transmission rate with higher reliability [23].

In view of increasing number of chaos applications, chaos generation from non-chaotic systems (or enhancing the existing chaos) with the inherent properties is still an important and challenging topic, which has also been referred to as anti-control of chaos [24] or chaotification [25]. In fact, before [24] and [25], reference [26] had used OGY idea to make the system trajectory tracking unstable orbit in transient chaos in order to maintain the trajectory in sustained state. A feedback chaos anti-control method for discrete systems was proposed by Lai and Chen [24]. Impulse control is applied to the discrete system, named heterogeneous cournot oligopoly model, for chaos generation through constant impulse signal [27]. Chaos generation from discrete system in the sense of Li-Yorke [24], [25], [28]–[31] was simpler than that from continuous time system, because, the dynamical analysis in continuous time system is more difficult. Numerous works have been reported to generate continuous time chaotic motion from non-chaotic systems. They include generating chaos using state feedback method [32]–[40], adaptive control method [41], [42], nonlinear time delay feedback control method [32], [33], linear time delay feedback method [34], [35] and piece-wise linear function feedback [43]–[45]. The resulting chaotic attractor can be single scroll [41], double scrolls [33], [36], [37], [40], [42], and multiple scrolls [34], [43]–[45]. Although there are many efforts to generate chaos using different methods, how to

Kun Tian is with the Shaanxi Key Laboratory of Complex System Control and Intelligent Information Processing, Xian University of Technology, Xian 710048, China. (e-mail: 1055490394@qq.com).

Celso Grebogi is with the Shaanxi Key Laboratory of Complex System Control and Intelligent Information Processing, Xian University of Technology, Xian 710048, China, and also with Institute for Complex Systems and Mathematical Biology, University of Aberdeen AB24 3UE, United Kingdom (grebogi@abdn.ac.uk).

Hai-Peng Ren is with the Shaanxi Key Laboratory of Complex System Control and Intelligent Information Processing, Xian University of Technology, Xian 710048, China. (Corresponding author e-mail: renhaipeng@xaut.edu.cn).

This paper was supported in part by the Shaanxi Provincial Special Support Program for Science and Technology Innovation Leader.

generate chaos with the required property and by considering the system constraints–for example, un-manipulated variables in the system state equations, or state constraints, is still a challenge and of the practical significance for different applications. Besides the methods based on continuous state feedback, an impulse control method was proposed to generate chaos from a stable periodic orbit of the nonlinear continuous system [46].

From control engineering perspectives, it is expected to unify chaos control and anti-control methods by adjusting parameters of the controller without altering the controller structure and the system configuration. Linear time delay feedback is shown to implement this aim by using it to control chaos [3] and to generate chaos [34]. The impulse control was shown to be able to control and synchronize chaos [47]–[51]. References [47]–[50] investigated the necessary conditions to guarantee the asymptotic stability of the synchronization error by using the Lyapunov theory. In [51], the negative Melnikov function was considered as a criterion for chaos suppression. In this paper, we explore the possibility to use the univariate impulse control to generate chaos from an originally non-chaotic system. Therefore, it is still interesting to investigate its ability to generate or to suppress chaos with more flexibility. To achieve this goal, in this work, we investigate chaos generation using univariate impulse control.

The univariate impulse control is a novel method for generating chaos, which is different from the previously existing methods for generating chaos, in the following aspects: (1) The impulse control regulates the system in an intermittent way, which is energy efficient and less state information dependent, contrary with continuous time control; (2) Comparing with all variables manipulation impulse method in [46] for generating chaotic attractor confining to the local region about the limit cycle, the features of this impulse control method are: first, the chaos generated by the proposed univariate impulse control is not confined to the local region of the limit cycle of the original system, which means that more flexibility is achieved by the proposed method; second, regulating a single state equation to simplify the control structure instead of the multiple manipulated variables in [46]. Compared with the multi-variate impulse control, the univariate impulse control faces with added challenge to implement the same task, because the manipulation dimension is decreased, and the freedom of the controller is reduced. But the univariate control is more in line with traditional control theory in which one variable or one parameter is manipulated. Moreover, for some special cases, the uncontrolled system to be controlled does not allow for the manipulation of multi-variables. In such a case, multi-variate impulse control is not applicable. Therefore, it is of practical significance to investigate the univariate impulse control for chaos generation. The univariate impulse control has a broadened application potential. This is in agreement with the traditional control theory in which a single parameter or a single variable is manipulated to achieve the desired control or, in this case, anti-control of chaos.

In this work, the periodic impulse is applied for chaotifying the non-chaotic system. In this proposed method, the non-chaotic Chen system is used as a paradigm to generate double-scroll attractors using impulse anti-control for the first time. The Chen circuit and an impulse circuit are built to validate the analytical results. The generated chaos characteristics are analysed by evaluating the Lyapunov exponent, power spectrum, bifurcation diagram, Poincaré mapping and Kaplan-Yorke dimension. Topological Horseshoe Lemma is used to confirm the existence of the chaotic attractor.

The organization of the remaining part of the paper is as follows. Section 2 gives the problem description and the general form of the controller. Section 3 gives simulation results of non-chaotic Chen system with the proposed impulse control, and the analysis of its dynamical properties, including the power spectrum, bifurcation diagram, Lyapunov exponent, Poincaré mapping, the coexisting attractors and Kaplan-Yorke dimension. Section 4 proves the existence of chaos in the attractor of the Chen system with impulse control using the Topological Horseshoe Lemma. Section 5 describes the building of an electrical circuit for the non-chaotic Chen system with the proposed impulse controller to demonstrate chaos generation in a circuit experiment. Section 6 gives the conclusions.

II. Chaos generation from non-Chaotic Chen system using impulse control

A. Problem statement

Consider a non-chaotic dynamical system in the form,

$$\dot{\mathbf{x}} = \mathbf{f}(\mathbf{x}), \tag{1}$$

where $\mathbf{x} \in R^n$, $\mathbf{f} \in R^n \to R^n$ is a smooth function, $\mathbf{x}(t_0)$ is the arbitrary initial condition of the system at time t_0.

A state feedback impulse controller is given by,

$$\begin{cases} \mathbf{u} = \mathbf{K} \cdot \mathbf{x}(t_\sigma^-), \ t = t_\sigma \\ \mathbf{u} = 0, \ t \neq t_\sigma, \end{cases} \tag{2}$$

where $\mathbf{u} \in R^n$ is the impulse control input to the system. The impulse is active at time t_σ satisfying $0 < t_1 < t_2 < ...$ and $\lim_{\sigma \to \infty} t_\sigma = \infty$. $\mathbf{K}$ is a matrix with only one non-zero element representing the gain matrix of the impulse control. The row with non-zero elements is the only one state variable to be manipulated. Although we refer $\mathbf{u}$ to be in R^n, in fact, only one component of $\mathbf{u}$ is non-zero.

In this paper, controller (2) is used to generate chaos from the non-chaotic system (1).

B. Univariate state feedback impulse control of non-chaotic Chen system

Using the non-chaotic Chen system [52] as example, we describe the paradigm of generating chaos in a non-chaotic system using univariate state feedback impulse control.

The Chen system is given by:

$$\begin{cases} \dot{x} = a(y - x) \\ \dot{y} = (c - a)x - xz + cy \ , \\ \dot{z} = xy - bz \end{cases} \tag{3}$$

where x, y and z are the state variables of the system and a, b and c are the parameters. In this paper, we consider that $a = 35$, $b = 3$ and $c = 18.5$, then the Chen system has stable equilibrium when no impulse control is applied.

To use a simple form, an impulse control is added to the y-variable of the system, as given by:

$$\begin{cases} \dot{x} = a(y - x) \\ \dot{y} = (c - a)x - xz + cy + u \\ \dot{z} = xy - bz \\ u = k \cdot y(t_\sigma^-),\ t = t_\sigma \\ u = 0,\ t \neq t_\sigma \end{cases}, \tag{4}$$

where u is the univariate state feedback impulse controller to manipulate state y using state y for feedback. During the time interval between two consecutive impulses, system (4) is the same as system (3). With the appropriate impulse interval $\delta = t_\sigma - t_{\sigma-1} (\sigma = 1, 2, ...)$ and impulse strength k, the stable equilibrium is converted to a chaotic attractor, whose dynamics is discussed in the next section.

Discussion 1. The proposed method can be extended to not only some other nonlinear systems with stable parameters, but also some linear systems. A linear system example has been described in Appendix A.

III. The Chaotic Attractor in the Non-Chaotic Chen System Generated by Univariate State Feedback Impulse Control

A. Chaos generated in a non-chaotic Chen system using impulse control

Consider system (4), when the parameters are $a = 35$, $b = 3$, $c = 18.5$ and $k = 0$, the system is non-chaotic. Trajectories starting from different attracting basins converge to one of the two stable equilibrium points $O_\pm$, as show in Fig. 1.

When the parameters of the impulse controller are the impulse interval $\delta = 0.4s$ and gain $k = 25$, a chaotic attractor is present in the controlled system, as shown in Fig. 2. It can be seen that the double-scroll attractor is generated in system (4) when univariate impulse control is activated. System (4) is invariant under the coordinate transformation $(x, y, z) \to (-x, -y, z)$. Therefore, system (4) is symmetric.

Multi-stability is the coexistence of multiple attractors, depending on different initial conditions for the same set of parameters, which shows the rich dynamical characteristics of the nonlinear system. With parameters $a = 35, b = 3$, and $c = 18.5$ for the system (4), the symmetry of the system leads to the appearance of double coexisting attractors. Two different initial conditions $[1, 1, 1]$ and $[-1, -1, 1]$ are taken to show the coexistence of period 1, single-scroll attractor and double-scroll attractor, as shown in Fig. 3(a), (b), and (c), respectively, as k varies.

B. Power spectrum

The power spectrum is calculated from the time series of x as shown in Figs. 2(d) and (e). From Fig. 2(e), the spectrum of x displays no apparent single peak, which is the feature of a chaotic signal. The other variables show similar power spectrum as that in Fig. 2(e), thus indicating the chaotic property of the signals.

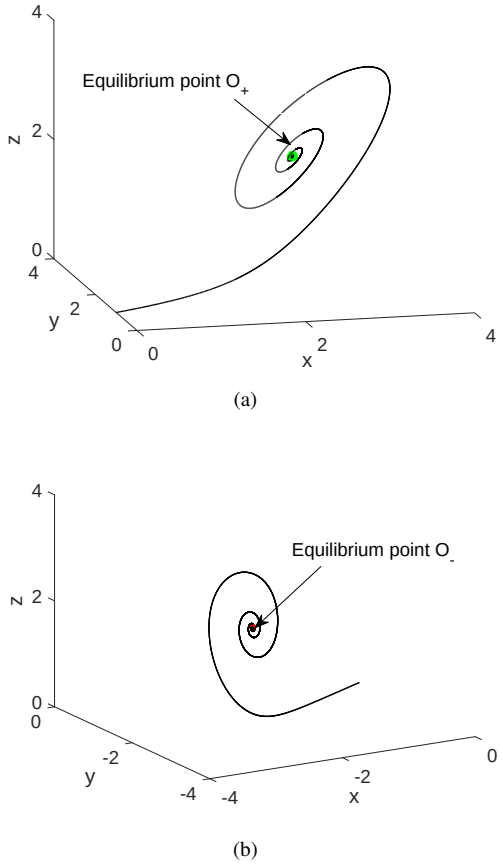

Fig. 1: The system state trajectories in phase space under different initial conditions located in different attracting basins of two equilibriums; (a) The trajectory approaches the equilibrium $O_+ (2.449, 2.449, 2)$ with the initial condition $[0, 1, 0]$; (b) The trajectory approaches the equilibrium $O_- (-2.449, -2.449, 2)$ with the initial condition $[0, -1, 0]$.

C. Bifurcation diagrams

We keep $\delta = 0.4s$, and use the impulse gain as the bifurcation parameter to obtain the bifurcation diagram given in Fig. 4(a). We keep the impulse gain k as 25, and use the parameter impulse interval as bifurcation parameter to derive the bifurcation diagram given in Fig. 4(b). We show the phase trajectory projection on the $x - y$ plane with different parameters in Fig. 5, from which we learn that the controlled system demonstrates complicated dynamics, including period-1 orbit, period-2 orbit, and multi-periodic orbit when the controller parameter varies, corresponding to the bifurcation diagram in Fig. 4(a).

D. Lyapunov exponents of the attractors

The estimation of the maximum Lyapunov exponent of the chaotic sequences is one of the fundamental measures in the study of dynamical system. This work adopts the method

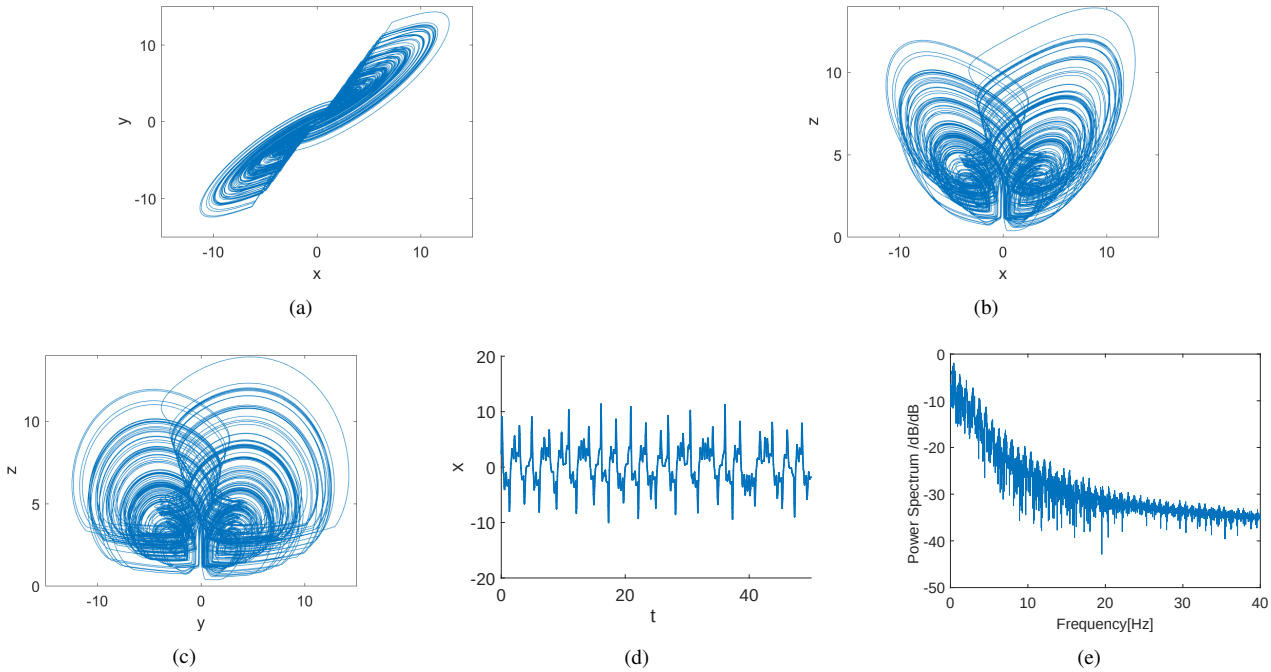

Fig. 2: The chaotic attractor generated in the Chen system using univariate state feedback impulse; (a) phase trajectory projection on the $x-y$ plane; (b) phase trajectory projection on the $x-z$ plane; (c) phase trajectory projection on the $y-z$ plane; (d) time series of x; (e) the power spectrum of time series x.

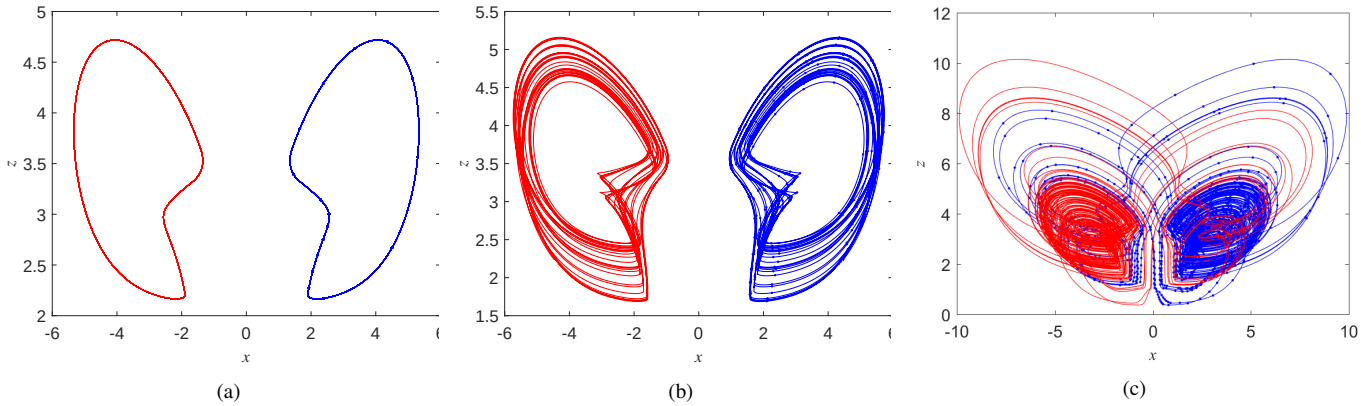

Fig. 3: Coexisting attractors in system (4) for trajectories starting from initial condition $\mathbf{x}(t_0) = [-1, -1, 1]$ plotted in red solid line and initial condition $\mathbf{x}(t_0) = [1, 1, 1]$ plotted in blue line with dots; (a) period-1 trajectories for $\delta = 0.4, k = 18.5$; (b) single-scroll attractor for $\delta = 0.4, k = 20$; (c) double-scroll attractor for $\delta = 0.4, k = 20.04$.

of BBA [53], to estimate the Lyapunov exponents from the observed time series. The BBA algorithm first reconstructs the phase space according to the time series of single variable using time-delay embedding method. Then, the least square method is used to extract the Jacobian matrix of the reconstructed dynamical system. Finally, the Lyapunov exponent spectrum is calculated from the eigenvalues of the Jacobian matrix. Using the BBA method, we obtain the Lyapunov exponent spectrum of the system as given in Fig. 6. It can be seen from Fig. 6 that there are three Lyapunov exponents whose values are 0.16, 0.03, and -1.129. The positive largest Lyapunov exponent indicates that the dynamics is chaotic.

E. Poincaré mapping

We define the Poincaré-section $P = \{(x, y, z) \in R^3 : z = 6\}$ with the normal vector $h = (0, 0, 1)$, as shown by the green plane in Fig. 7. The plane intersects the trajectory and its mapping points on the section P, as shown in Fig. 8 in a new coordinate, which shows some continuous points. From Fig. 8, we know that the system is chaotic.

F. Kaplan-Yorke dimension

According to the Kaplan-York conjecture, D_{KY} is calculated by,

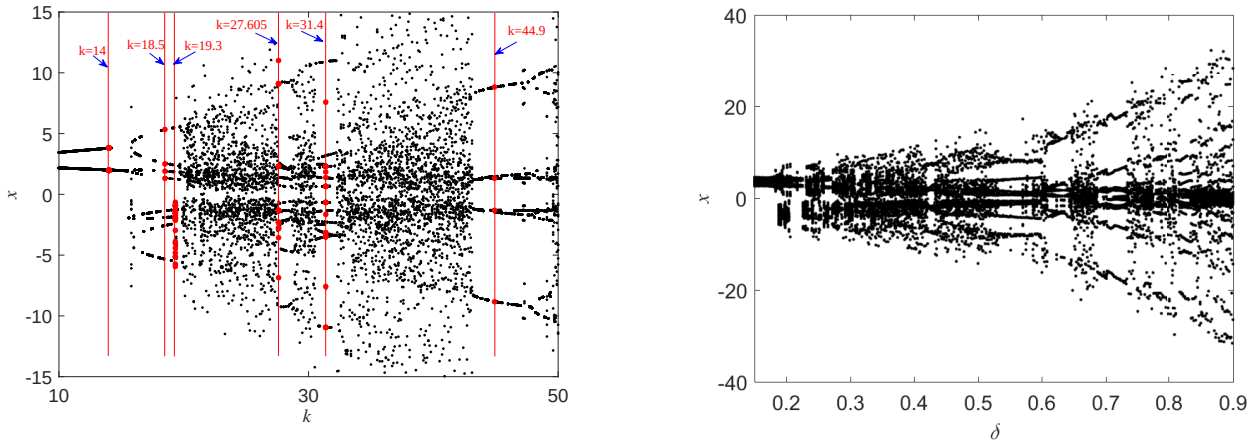

(a) (b)

Fig. 4: The bifurcation diagram of x state as: (a) the impulse strength k is varied from 10 to 50 with the impulse interval $\delta = 0.4s$; (b) the impulse interval δ is varied from 0.15 to 0.9 with the impulse strength $k = 25$.

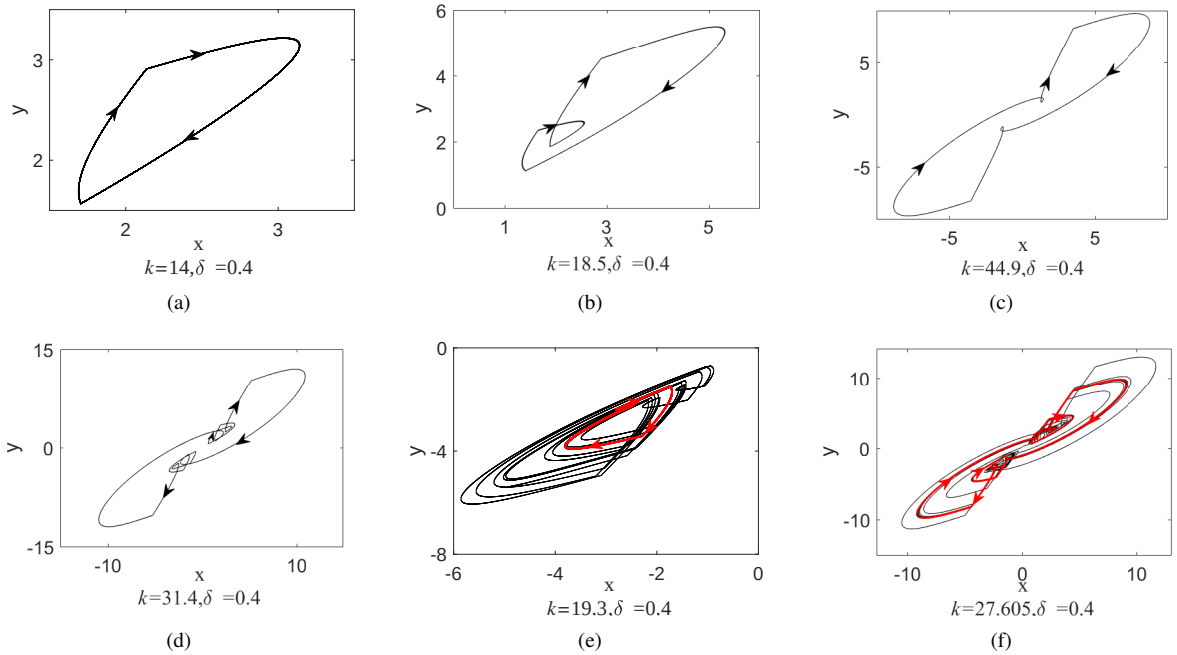

(a) (b) (c) (d) (e) (f)

Fig. 5: The phase trajectory projection with different parameters on the $x-y$ plane; (a)$k = 14, \delta = 0.4$; (b)$k = 18.5, \delta = 0.4$; (c)$k = 44.9, \delta = 0.4$; (d)$k = 31.4, \delta = 0.4$; (e)$k = 19.3, \delta = 0.4$; (f)$k = 27.605, \delta = 0.4$.

$$D_{KY} = S + \frac{\sum_{i=1}^{s} L_i}{|L_{i+1}|}, \tag{5}$$

where $L_i (i = 1, 2, 3, ..., n)$ is the Lyapunov exponents of the n-order system, S represents the number of positive Lyapunov exponents. Therefore, the Kaplan-Yorke dimension of system (4), using the proposed anti-control method with control parameters $k = 25$ and $\delta = 0.4$, is $D_{KY} = 2.17$.

IV. Horseshoe in the Chen System with Impulse Control

A. Topological horseshoe

The topological Horseshoe Lemma provides conditions for the existence of a topological horseshoe, which is used as a method for the proof of existing chaos.

Let X be a metric space; $D \in X$ is a compact subset; $f : D \to X$ is a diffeomorphism; and there exists mutually disjoint compact subsets $D_1, ..., D_m$ of D such that $f|D_i$ is continuous. According to [54], we have the following definitions and Lemma.

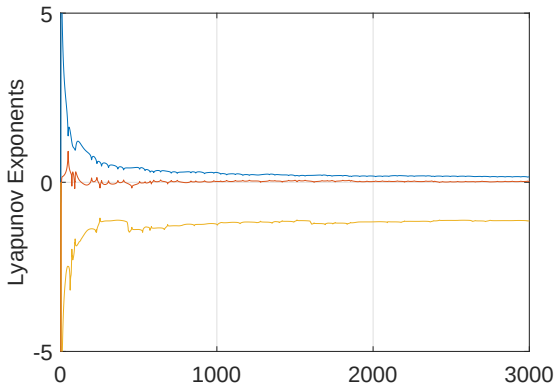

Fig. 6: Lyapunov exponent spectrum of the Chen system after the univariate impulse anti-control is applied.

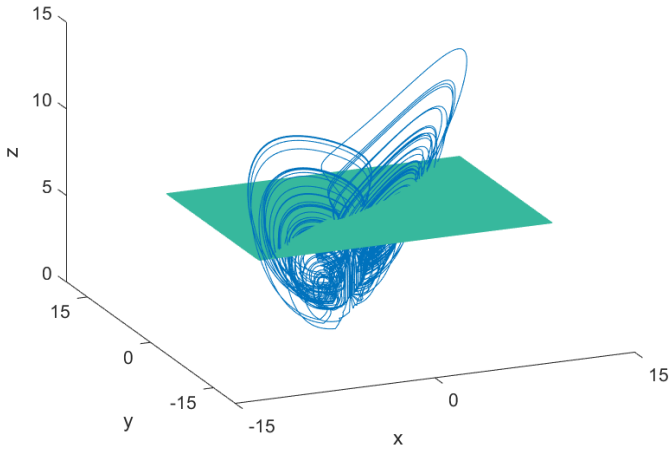

Fig. 7: Poincaré section of the Chen system with impulse anti-control.

Definition 1: For each $1 \leqslant i \leqslant m$, let D_i^1 and D_i^2 be two fixed disjoint compact subsets of D_i. A subset l of D_i is said to connect D_i^1 and D_i^2 if $l \cap D_i^1 \neq \emptyset$ and $l \cap D_i^2 \neq \emptyset$, and we denote this by $D_i^1 \overset{l}{\leftrightarrow} D_i^2$.

Definition 2: If l contains a connected subset l' such that $D_j^1 \overset{f(l')}{\leftrightarrow} D_j^2$, we define that $f(l)$ across D_j with D_j^1 and D_j^2, and it is denoted as $f(l) \mapsto D_j$. If $f(l) \mapsto D_j$ for every connected subset $l \subset D_i$ with $D_i^1 \overset{l}{\leftrightarrow} D_i^2$ is satisfied, $f(D_i)$ is suitably across D_j and it is denoted as $f(D_i) \mapsto D_j$.

Lemma 1: If $f^p(D_1) \mapsto D_1$, $f^p(D_1) \mapsto D_2$, and $f^q(D_2) \mapsto D_1$, then there exists a compact invariant set $J \subset D$ such that $f^{2p+q}|J$ is semiconjugate to two-shift dynamics, and $ent(f) \geqslant (1/2p+q)\log 2$.

B. Topological horseshoes in Chen system with impulse anti-control

The existence of horseshoe in the dynamical systems is a proof of existence of chaos. We present the construction of the topological horseshoe in this sub-section. To select suitable quadrilaterals in the Poincaré section satisfying across conditions is complicated.

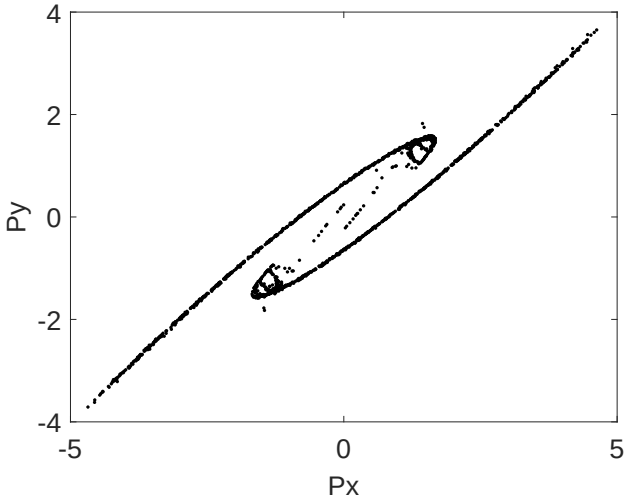

Fig. 8: The Poincaré mapping points on P.

We select a quadrangle $A_1B_1C_1D_1$ in Fig. 8, whose vertex coordinates are $A_1 = [0.4, 0.002, 6]$, $B_1 = [0.427, 0.0288, 6]$, $C_1 = [0.823, -0.167, 6]$, $D_1 = [0.781, -0.209, 6]$, as shown with the red quadrangle in Fig. 9(a) in the Pioncaré plane. Quadrangles $A_1B_1C_1D_1$ is mapped as $A_1'B_1'C_1'D_1' = f^2(A_1B_1C_1D_1)$ through twice Poincaré mapping, and $A_1'B_1'C_1'D_1'$ intersects $A_1B_1C_1D_1$, as shown in Fig. 9(b).

We select a similar quadrangle $A_2B_2C_2D_2$ with the coordinates of the four vertices as $A_2 = [0.373, -0.033, 6]$, $B_2 = [0.395, -0.003, 6]$, $C_2 = [0.77, -0.239, 6]$, $D_2 = [0.7, -0.286, 6]$, as shown by the green quadrangle in the Fig. 9(a). The twice mapping $A_2'B_2'C_2'D_2' = f^2(A_2B_2C_2D_2)$ is intersecting $A_1B_1C_1D_1$, and $A_1'B_1'C_1'D_1'$ is intersecting $A_2B_2C_2D_2$, as shown in Fig. 9(c).

Upon the above simulation results, there exist two quadrangles satisfying $f^2(A_1B_1C_1D_1) \mapsto A_1B_1C_1D_1$, $f^2(A_1B_1C_1D_1) \mapsto A_2B_2C_2D_2$ and $f^2(A_2B_2C_2D_2) \mapsto A_1B_1C_1D_1$. According to the Lemma 1, there exists a compact invariant set $J \subset D$ such that $f^6|J$ is semiconjugate to two-shift dynamics, and $ent(f) \geqslant (1/6)\log 2 > 0$. Consequently, there exists chaos in the sense of topological horseshoe in system (4).

V. Circuit Design

To implement the Chen circuit, FPGA [55] or FPAA [56] is an option, which has advantages, like easy implementation, easy reconfiguration of the parameters, etc. However, these digital implementations have to numerically integrate the differential equations, which are the same as done in the computer simulations, although they in fact implement the circuit using an integrated circuit chip. Therefore, it has the same issues as those demonstrated in computer simulations, like the numerical precision, trunk error, etc. Although the

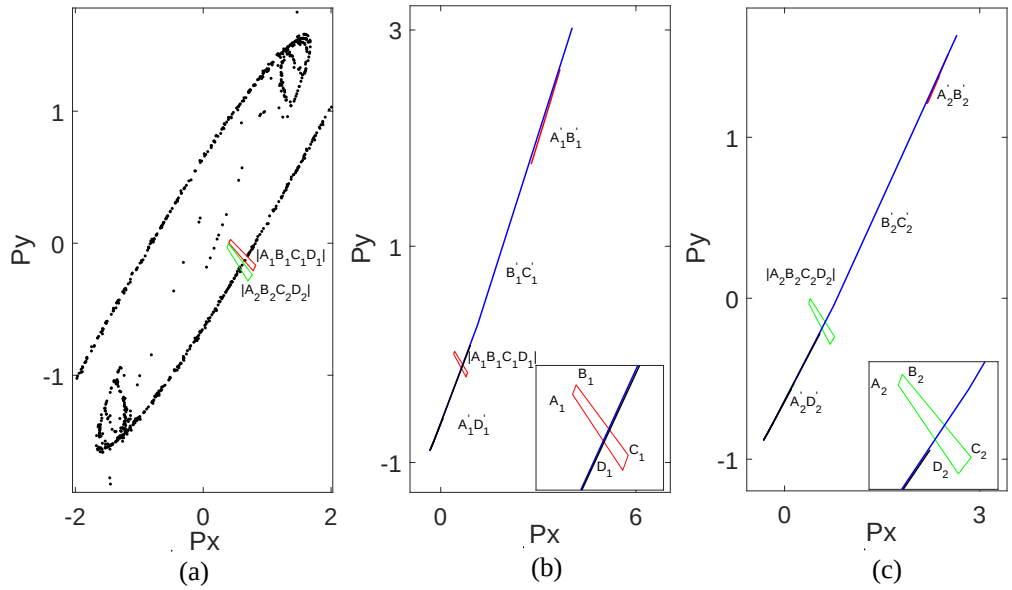

Fig. 9: The quadrangles $A_1B_1C_1D_1$, $A_2B_2C_2D_2$ and their map f^2; (a) Global view of the position $A_1B_1C_1D_1$ and $A_2B_2C_2D_2$; (b) The image of $A_1'B_1'C_1'D_1'$, where $A_1'B_1' = f^2(A_1B_1)$, $B_1'C_1' = f^2(B_1C_1)$, $C_1'D_1' = f^2(C_1D_1)$ and $A_1'D_1' = f^2(A_1D_1)$; (c) The image of $A_2'B_2'C_2'D_2'$, where $A_2'B_2' = f^2(A_2B_2)$, $B_2'C_2' = f^2(B_2C_2)$ and $A_2'D_2' = f^2(A_2D_2)$.

analog circuit implementation is complex, for example, the difficulty in changing parameters, parasite parameter, and inaccurate parameter, it still demonstrates the properties of the practical circuit, which is not a simulation. To further validate the chaotic attractors generated by the proposed impulse controller, we designed an experimental circuit with analog operational amplifier. The circuit is composed of two blocks, the non-chaotic Chen circuit and the impulse controller. The circuit consists mainly of operation amplifiers (LF347N), multipliers (AD633), and a timer (555). In the circuit design, the multiplication factor of AD633 is 0.1. Therefore, we adjust the magnification of the nonlinear factors of the Chen system model as Eq. (6).

The schematic circuit diagram of the circuit implementation is shown in Fig. 10, the corresponding components parameters are summarized in Table I. The circuit simulation is carried out using PSIM. The impulse controller block is consisted of op-amps $U_8 \sim U_{10}$, 555 timer and bilateral switch CD4066. Due to the saturation of the CD4066 is $\pm 5V$, the signal amplitude of y is firstly decreased using U_8, then recovers the amplitude through U_9 and U_{10} at the moment that the CD4066 is on-state when the timer 555 output is on high level. In such a way, the impulse control signal is generated. According to the circuit schematic diagram, the system parameters corresponding to the circuit component are given in Eq. (7). The detailed derivation of Eq. (7) has given in Appendix B.

$$\begin{cases} \dot{x} = a(y - x) \\ \dot{y} = (c - a)x - 10xz + cy + u \\ \dot{z} = 10xy - bz \\ u = k \cdot y(t_\sigma^-),\ t = t_\sigma \\ u = 0,\ t \neq t_\sigma \end{cases}. \tag{6}$$

$$\begin{aligned} a &= \frac{R_3(R_1 + R_4)}{R_1R_5C_1(R_2 + R_3)}; \\ c - a &= -\frac{R_7R_8R_{11}R_{14}R_{18}R_{19}\,(R_9 + R_{12})\,(R_{15} + R_{16})}{R_6R_9R_{13}R_{15}R_{20}C_2\,(R_8R_{10} + R_{10}R_{11} + R_8R_{11})\,(R_{17}R_{18} + R_{17}R_{19} + R_{18}R_{19})}; \\ c &= \frac{R_{10}R_{11}R_{14}R_{18}R_{19}\,(R_9 + R_{12})\,(R_{15} + R_{16})}{R_9R_{13}R_{15}R_{20}C_2\,(R_8R_{10} + R_{10}R_{11} + R_8R_{11})\,(R_{17}R_{18} + R_{17}R_{19} + R_{18}R_{19})}; \\ b &= \frac{(R_{28} + R_{31})R_{30}}{(R_{29} + R_{30})R_{28}R_{32}C_3}. \end{aligned} \tag{7}$$

The impulse control gain is,

$$k = \frac{R_{22}R_{25}R_{27}}{R_{21}R_{24}R_{26}R_{20}C_2}. \tag{8}$$

By adding the univariate impulse controller to Chen circuit, we obtain double-scroll attractors in the experiment, as shown in Fig. 11. Figures 11(a)-(c) represent the phase space trajectories projected into the $x-y$, $x-z$ and $y-z$ planes, respectively.

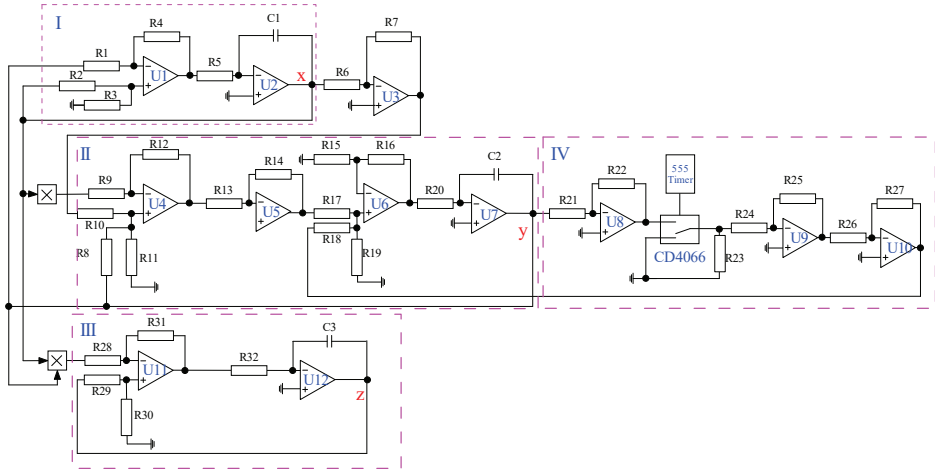

Fig. 10: Circuit diagram of the Chen system with impulse anti-control on y-variable.

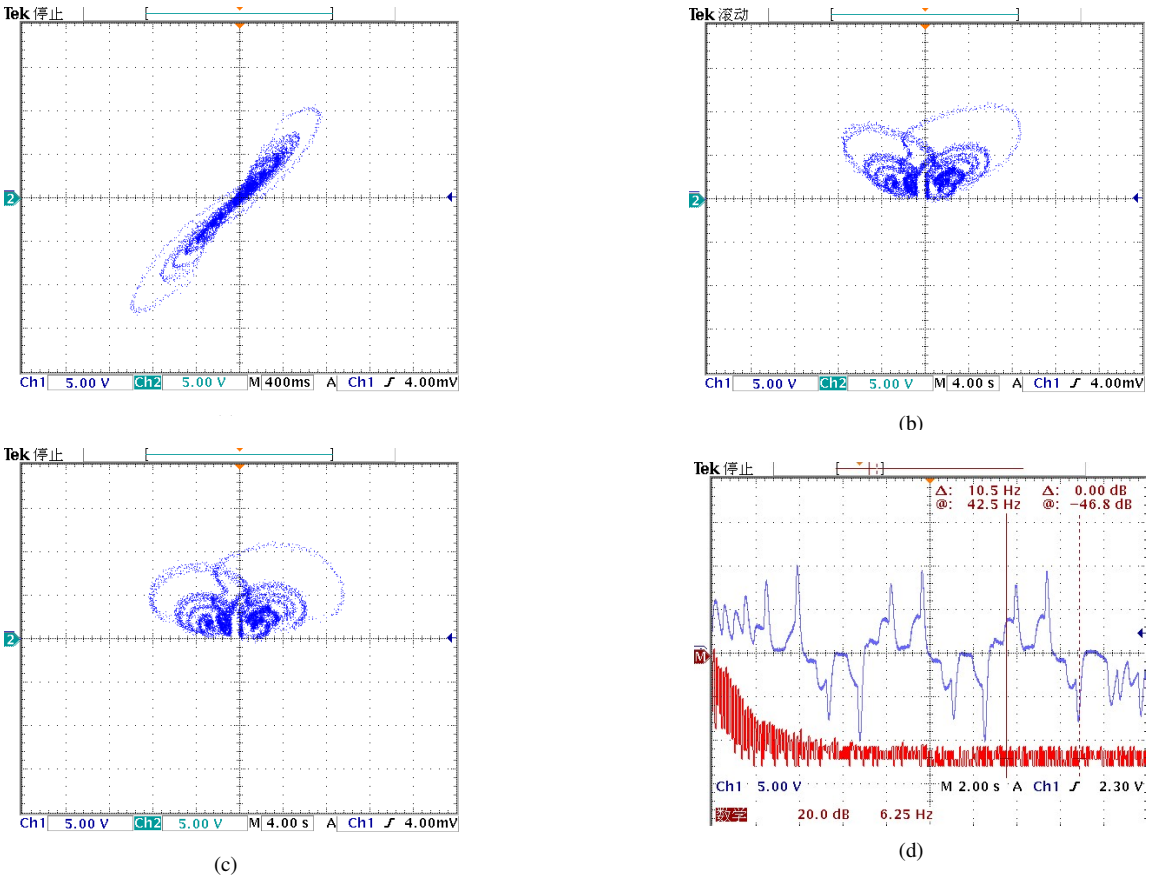

Fig. 11: The experimental results of the attractor in the Chen system with impulse anti-control on the y-variable; (a) attractor projection on $x-y$ plane; (b) attractor projection on $x-z$ plane; (c) attractor projection on $y-z$ plane; (d) the time domain waveform of $x(t)$ and its power spectrum.

TABLE I: Circuit component parameters

Component	Value
$R_1, R_2, R_3, R_4, R_6, R_7, R_{13}, R_{14}$, $R_{15}, R_{17}, R_{18}, R_{19}, R_{28}, R_{29}, R_{31}$	$10k\Omega$
R_5	$2.86M\Omega$
R_8	$16.5k\Omega$
R_9	$3k\Omega$
R_{10}	$18.5k\Omega$
R_{11}	$60k\Omega$
$R_{12}, R_{21}, R_{24}, R_{26}, R_{27}$	$1k\Omega$
R_{16}	$20k\Omega$
R_{20}	$3.33M\Omega$
R_{22}	280Ω
R_{23}	500Ω
R_{25}	$3k\Omega$
R_{30}	1765Ω
R_{32}	$10M\Omega$
C_1, C_2, C_3	$10pF\Omega$

Fig. 11(d) represents the time domain waveform of $x(t)$ and its power spectrum. From Fig. 11, the experiment results are consistent with the simulation results given in Fig. 2, and validates the effectiveness of the chaos generation method.

VI. Conclusions

This paper presents a chaos generation method using univariate state feedback impulse controller. We use the non-chaotic Chen system as paradigm to show the effectiveness and veracity of our method. To explore the basic dynamical characteristics of the new attractors, the power spectrum, bifurcation diagrams and the largest Lyapunov exponent are analysed in this paper. We also designed a circuit to validate our method in the double-scroll attractor experimentally. The numerical simulations are consistent with the experimental results. Moreover, the topological horseshoe proves that the attractor is chaotic.

The method in this paper offers a flexibility approach when intermittent and energy efficient controls are preferable to create chaos. The exploration of a possible principle to determine the parameter range for chaos generation using univariate impulse control and the application of the chaos generated by the proposed impulse control are the future tasks.

Appendix A

The proposed univariate impulse control method is capable for generating chaos from the non-chaotic linear systems, such as the linear system given by,

$$\begin{cases} \dot{x}_1 = -2x_2 \\ \dot{x}_2 = x_1 \\ \dot{x}_3 = 1 + x_2 - 2x_3 \end{cases}. \tag{9}$$

If we introduce the proposed impulse controller with the nonlinear state feedback given by $u = 5x_3^2(t_\sigma^-)$ with the impulse interval $\delta = 0.03$ to x_2-variable, the proposed univariate impulse controller is capable of generating chaos from system (9), as shown in Fig. 12 for this impulse control system.

The bifurcation diagram of impulse strength k_2 are given in Fig. 13.

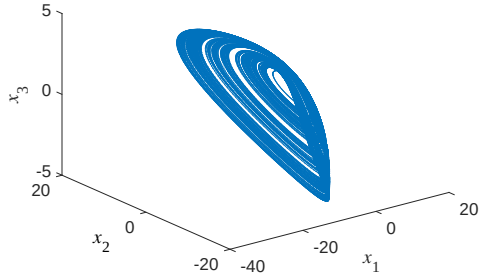

Fig. 12: The phase trajectory of the linear system (9) with univariate impulse controller.

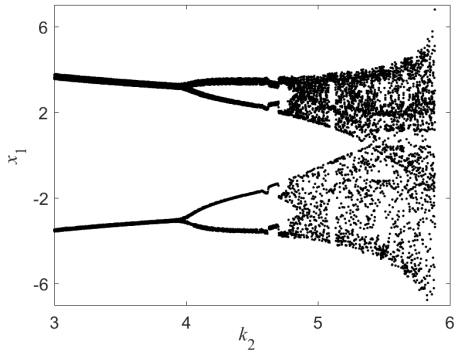

Fig. 13: The bifurcation diagram of state of x_1 as the impulse strength k_2 is varied from 3 to 5.8 with the impulse interval $\delta = 0.03$.

Appendix B

We used PSIM software to simulate the circuit, the print board is designed using Altium Designer software. Equation (6) is the final expression of the circuit, which can be derived using the basic circuit principle like Kirchchoff's laws, as given in the following.

From Fig. 14, u_x is given by,

$$\begin{cases} \dfrac{(R_1 + R_4)\, R_3}{(R_2 + R_3)\, R_1} u_x - \dfrac{u_y}{R_1} = u_1 \\ u_x = -\dfrac{1}{R_5 C_1} \displaystyle\int u_1 dt \end{cases}. \tag{10}$$

Equation (10) can be rewritten as,

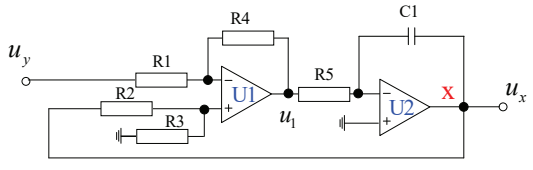

Fig. 14: Part I of the circuit diagram in Fig. 10.

$$-\frac{(R_1+R_4)R_3}{(R_2+R_3)R_1R_5C_1}u_x+\frac{1}{R_1R_5C_1}u_y=\dot{u}_x. \tag{11}$$

From Fig. 15, u_y is given by:,

$$\begin{cases} u_4=\dfrac{(R_9+R_{12})R_8R_{10}R_{11}}{R_9(R_8R_{10}+R_8R_{11}+R_{10}R_{11})}\left(\dfrac{u_y}{R_8}-\dfrac{R_7u_x}{R_6R_{10}}\right)-\dfrac{R_{12}u_{xz}}{R_9} \\ u_5=-\dfrac{R_{14}}{R_{13}}u_4 \\ u_6=\dfrac{(R_{15}+R_{16})R_{19}(u_5R_{18}+uR_{17})}{R_{15}(R_{17}R_{18}+R_{18}R_{19}+R_{17}R_{19})} \\ u_y=-\dfrac{1}{R_{20}C_2}\displaystyle\int u_6dt \end{cases}. \tag{12}$$

Equation (12) can be rewritten as,

$$\begin{aligned} \dot{u}_y=&\frac{R_{10}R_{11}R_{14}R_{18}R_{19}(R_9+R_{12})(R_{15}+R_{16})}{R_9R_{13}R_{15}R_{20}C_2(R_8R_{10}+R_{10}R_{11}+R_8R_{11})(R_{17}R_{18}+R_{17}R_{19}+R_{18}R_{19})}u_y \\ &-\frac{R_7R_8R_{11}R_{14}R_{18}R_{19}(R_9+R_{12})(R_{15}+R_{16})}{R_6R_9R_{13}R_{15}R_{20}C_2(R_8R_{10}+R_{10}R_{11}+R_8R_{11})(R_{17}R_{18}+R_{17}R_{19}+R_{18}R_{19})}u_x \\ &-\frac{R_{12}R_{14}R_{18}R_{19}(R_{15}+R_{16})}{R_9R_{13}R_{15}R_{20}C_2(R_{17}R_{18}+R_{17}R_{19}+R_{18}R_{19})}u_{xz}. \end{aligned} \tag{13}$$

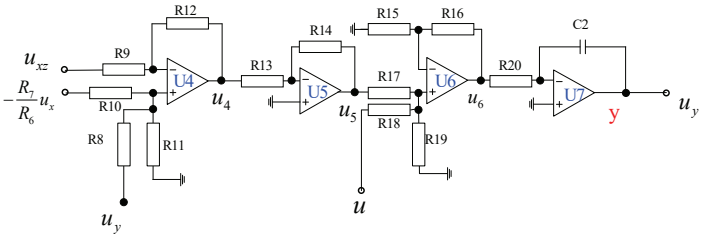

Fig. 15: Part II of the circuit diagram in Fig. 10.

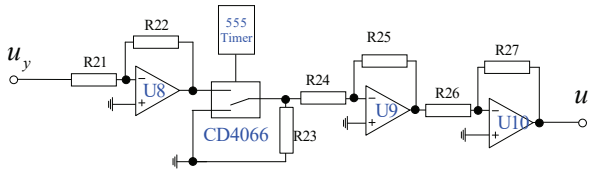

Fig. 17: Part IV of the circuit diagram in Fig. 10.

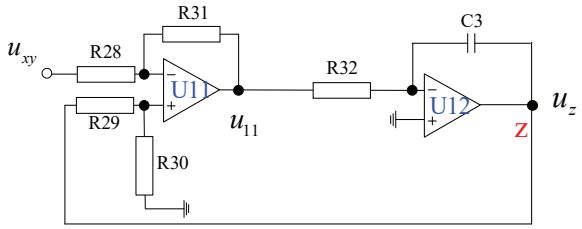

Fig. 16: Part III of the circuit diagram in Fig. 10.

From Fig. 16, u_z is given by:

$$\begin{cases} u_{11}=\dfrac{(R_{28}+R_{31})R_{30}}{R_{28}(R_{29}+R_{30})}u_z-\dfrac{R_{31}}{R_{28}}u_{xy} \\ u_z=-\dfrac{1}{R_{32}C_3}\displaystyle\int u_{11}dt \end{cases}. \tag{14}$$

Equation (14) can be rewritten as,

$$\dot{u}_z=\frac{R_{31}}{R_{28}R_{32}C_3}u_{xy}-\frac{(R_{28}+R_{31})R_{30}}{R_{28}R_{32}C_3(R_{29}+R_{30})}u_z. \tag{15}$$

From Fig. 17, u is given by:

$$u=-\frac{R_{22}R_{25}R_{27}}{R_{21}R_{24}R_{26}}u_y. \tag{16}$$

From equations (11), (13), (15) and (16), we can obtain the circuit parameters given by equations (6), (7) and (8).

REFERENCES

[1] E. N. Lorenz, "Deterministic nonperiodic flow," *J. Atmospheric Sci.*, vol. 20, no. 2, pp. 130-141, Mar. 1963.

[2] E. Ott, C. Grebogi and J. A. Yorke, "Controlling chaos," *Phys. Rev. Lett.*, vol. 64, no. 11, pp. 1196-1199, Mar. 1990.

[3] K. Pyragas, "Continuous control of chaos by self-controlling feedback," *Phys. Lett. A*, vol. 170, no. 6, pp. 421-428, Nov. 1992.

[4] G. R. Chen, "Controlling Chua's global unfolding circuit family," *IEEE Trans. Circuits Syst. I, Fundam. Theory Appl.*, vol. 40, no. 11, pp. 829-832, Nov. 1993.

[5] M. T. Yassen, "Chaos control of Chen chaotic dynamical system," *Chaos Soliton. Fract.*, vol. 15, no. 2, pp. 271-283, Jan. 2003.

[6] Z. X. Zhou, C. Grebogi and H. P. Ren, "Parameter impulse control of chaos in crystal growth process," *J. Cryst. Growth*, vol. 563, no. 1, pp. 126079, Jun. 2021.

[7] I. Ahmad, "A Lyapunov-based direct adaptive controller for the suppression and synchronization of a perturbed nuclear spin generator chaotic system," *Appl. Math. Comput.*, vol. 395, no. 15, pp. 125858, Apr. 2021.

[8] H. Li, B. Zhang, Z. Li, W. A. Halang and G. R. Chen, "Controlling DC-DC converters by chaos-based pulse width modulation to reduce EMI," *Chaos Soliton. Fract.*, vol. 42, no. 3, pp. 1378-1387, Nov. 2009.

[9] H. P. Ren, C. Bai, Q. J. Kong, S. M. Baptista and C. Grebogi, "A chaotic spread spectrum system for underwater acoustic communication," *Phys. A*, vol. 478, no. 15, pp. 77-92, Jul. 2017.

[10] C. Bai, H. P. Ren, S. M. Baptista and C. Grebogi, "Digital underwater communication with chaos," *Commun. Nonlinear Sci. Numer. Simul.*, vol. 73, no. 15, pp. 14-24, Jul. 2019.

[11] H. P. Ren, "A method of realizing single direction chaotic rotation speed of permant magnet synchronous motor is provided powered by a three-phase full bridge inverter," *Amer. Patent Appl*, PCT/CN2016/073418, Mar. 19, 2019.

[12] Z. Wang and K. T. Chau, "Anti-control of chaos of a permanent magnet DC motor system for vibratory compactors," *Chaos Soliton. Fract.*, vol. 36, no. 3, pp. 694-708, May. 2008.

[13] D. Gu, Z. Liu, C. Xu, J. Li, C. Tao and Y. Wang, "Solid-liquid mixing performance in a stirred tank with a double punched rigid-flexible impeller coupled with a chaotic motor," *Chem. Eng. Process*, vol. 118, pp. 37-46, Aug. 2017.

[14] L. X. Li, Y. X. Yang, H. P. Peng and X. D. Wang, "An optimization method inspired by chaotic ant behavior," *Int J. Bifurcation Chaos*, vol. 16, no. 8, pp. 2351-2364, Nov. 2006

[15] A. M. S. Mahdy, M. Higazy, K. A. Gepreel and A. A. A. El-dahdouh, "Optimal control and bifurcation diagram for a model nonlinear fractional SIRC," *Alex. Eng. J*, vol. 59, no. 5, pp. 3481-3501, Otc. 2020.

[16] H. A. Hefny and S. S. Azab, "Chaotic particle swarm optimization," *International Conference on Informatics and Systems INFOS 2010*, Giza, Egypt, 2010.

[17] A. Apostolos, S. Dimitris, L. Laurent, A. L. Valerio, C. Pere, F. Ingo, G. O. Jordi, R. M. Claudio, P. Luis and K. A. Shore, "Chaos-based communications at high bit rates using commercial fiber-optic links," *Nature*, vol. 438, no. 7066, pp. 343-346, Nov. 2005

[18] "IEEE Std 802.15.6-2012." *IEEE standard for local and metropolitan area networks-Part 15.6: Wireless body area networks*, 2012.

[19] N. J. Corron and J. N. Blakely, "Chaos in optimal communication waveforms," *Proceedings of the Royal Society A*, vol. 471, no. 2180, pp. 20150222, Aug. 2015.

[20] H. P. Ren, M. S. Baptista and C. Grebogi, "Wireless communication with chaos," *Phys. Rev. Lett.*, vol. 110, no. 18, pp. 184101, May. 2013.

[21] J. L. Yao, C. Li, H. P. Ren and C. Grebogi, "Chaos-based wireless communication resisting multipath effects," *Phys. Rev. E*, vol. 96, no. 3, pp. 032226, Sep. 2017.

[22] H. P. Ren, H. P. Yin, C. Bai and J. L. Yao, "Performance improvement of chaotic baseband wireless communication using Echo State Network," *IEEE Trans. Commun.*, vol. 68, no. 10, pp. 6525-6536, Oct. 2020.

[23] C. Bai, H. P. Ren and G. Kolumban, "Double-sub-streams Mary Differential Chaos Shift Keying Wireless Communication System using Chaotic Shape-Forming Filter," *IEEE Trans. Circuits Syst. I. Reg. Papers*, vol. 67, no. 10, pp.3574-3587, Oct. 2020.

[24] G. R. Chen and D. Lai, "Feedback anticontrol of discrete chaos," *Int. J. Bifurcation Chaos*, vol. 8, no. 7, pp. 1585-1590, May. 1998.

[25] X. F. Wang and G. R. Chen, "Chaotification via arbitrarily small feedback controls: Theory, method, and applications," *Int. J. Bifurcation Chaos*, vol. 10, no. 3, pp. 549-570, Apr. 2000.

[26] Y. C. Lai, C. Gregobi, "Coverting transient chaos into sustained chaos by feedback control," *Phys. Rev. E*, vol. 49, no. 2, pp. 1094, Feb. 1994.

[27] M. Lampart and A. Lampartova, "Chaos Control and Anti-Control of the Heterogeneous Cournot Oligopoly Model," *Mathematics*, vol. 8, no. 10, pp. 1670, Sep. 2020.

[28] G. R. Chen and D. J. Lai, "Feedback control of Lyapunov exponents for discrete-time dynamical systems," *Int. J. Bifurcation Chaos*, vol. 6, no. 7, pp. 1341-1349, Sep. 1996.

[29] X. F. Wang and G. R. Chen, "On feedback anticontrol of discrete chaos," *Int. J. Bifurcation Chaos*, vol. 9, no. 7, pp. 1435-1441, Jul. 1999

[30] G. R. Chen, "Chaotification via Feedback: The discrete case. Chaos control." *Berlin: Springer*, 2003.

[31] W. Liang and Z. H. Zhang, "Anti-control of chaos for first-order partial difference equations via sine and cosine functions," *Int. J. Bifurcation Chaos*, vol. 29, no. 10, pp. 1950140, Feb. 2019.

[32] X. F. Wang, G. R. Chen and X. H. Yu, "Anticontrol of chaos in continuous-time systems via time-delay feedback," *Chaos*, vol. 10, no. 4, pp. 771-779, Dec. 2001.

[33] X. F. Wang, G. Q. Guo, K. S. Tang, K. F. Man and Z. F. Liu, "Generating chaos in Chuas circuit via time delay feedback," *IEEE Trans. Circuit Syst. I. Reg. Papers*, vol. 48, no. 9, pp. 1151-1156, Sep. 2001.

[34] H. P. Ren, C. Bai, K. Tian and C. Grebogi, "Dynamics of delay induced composite multi-scroll attractor and its application in encryption," *Int. J. Non-Linear Mech.*, vol. 94, pp. 334-342, Sep. 2017.

[35] H. P. Ren, D. Liu and C. Z. Han, "Anticontrol of chaos via direct time delay feedback," *Acta. Phys. Sinica,(in Chinese)*, vol. 55, no. 6, pp. 2694-2701, Jun. 2006.

[36] A. Chen, J. N. Lu, J. H. Lü and S. M. Yu, "Generating hyperchaotic Lü attractor via state feedback control," *Phys. A*, vol. 364, no. 15, pp. 103-110, May. 2006.

[37] T. G. Gao, Z. Q. Chen, Q. L. Gu and Z. Z. Yuan, "A new hyper-chaos generated from generalized Lorenz system via nonlinear feedback," *Chaos Soliton. Fract.*, vol. 35, no. 2, pp. 390-397, Jan. 2008.

[38] M. Borah and B. K. Roy, "Systematic construction of high dimensional fractional-order hyperchaotic systems," *Chaos Soliton. Fract.*, vol. 131, pp. 109539, Feb. 2020.

[39] D. Ghosh, A. Mukherjee, N, R. Das and B. N. Biswas, "Generation and control of chaos in a single loop optoelectronic oscillator," *Optik*, vol. 165, pp. 275-287, Jul. 2018.

[40] L. J. Ontanon-Garcła and E. Campos-Cantn, "Preservation of a two-wing Lorenz-like attractor with stable equilibria," *J. Franklin Inst.*, vol. 350, no. 10, pp. 2867-2880, Dec. 2013.

[41] M. Javier and T. Carlos, "Adaptive chaotification of robot manipulators via neural networks with experimental evaluations," *Neurocomputing*, vol. 182, no. 19, pp.56-65, Mar. 2016.

[42] E. Asiain and R. Garrido, "Anti-chaos control of a servo system using nonlinear model reference adaptive control, " *Chaos Soliton. Fract.*, vol. 143, pp. 110581, Feb, 2021.

[43] R. J. Escalante-Gonzalez, E. Campos-Canton and M. Nicol. "Generation of multi-scroll attractors without equilibria via piecewise linear systems, " *Chaos*, vol. 27, pp. 053109, May, 2017.

[44] N. Wang, C. Q. Li, H. Bao, M. Mo and B. C. Bao. "Generating multi-scroll Chua's attractors via simplified piecewise-linear Chua's Diode, " *IEEE Trans. Circuits Syst. I, Reg. Papers*, vol. 66, pp. 4767-4779, Dec, 2019.

[45] N. Wang and G. S. Zhang. "Parametric control for multi-scroll attractor generation via nested sine-PWL function, " *IEEE Trans. Circuits Syst., II, Exp. Briefs*, vol. 68, pp. 1033-1037, March, 2021.

[46] L. Yang, Z. R. Liu and G. R. Chen, "Chaotifying a continuous-time system via impulsive input," *Int. J. Bifurcation Chaos*, vol. 12, no. 5, pp. 1121-1128, Oct. 2002.

[47] D. Chen, J. Sun, C. Huang, "Impulsive control and synchronization of general chaotic system," *Chaos Soliton. Fract.*, vol. 28, no. 1, pp. 213-218, Apr. 2006.

[48] C. D. Li, X. F. Liao, X. F. Yang and T. W. Huang, "Impulsive stabilization and synchronization of a class of chaotic delay systems," *Chaos*, vol. 15, no. 4, pp. 043103, Dec. 2005.

[49] K. Tian, H. P. Ren, C. Grebogi, "Rössler-Network with time delay: Univariate impulse pinning synchronization," *Chaos*, vol. 30, no. 12, (to appear) 2020. DOI: 10.1063/5.0017295

[50] K. Tian, C. Bai, H. P. Ren and C. Grebogi, "Hyperchaos synchronization using univariate impulse control," *Phys. Rev. E*, vol. 100, no. 5, pp. 052215, Nov. 2019.

[51] Z. X. Zhou, C. Grebogi and H. P. Ren, "Impulse control of chaos in the flexible shaft rotating-lifting system of the mono-silicon crystal puller," *arXiv*, 2003.05144, 2020.

[52] G. R. Chen and T. S. Ueta, "Yet another chaotic attractor," *Int. J. Bifurcation Chaos*, vol. 9, no. 7, pp. 1465-1466, Mar. 1999.

[53] R. Brown, P. Bryant, H. D. I. Abarbanel, "Computing the Lyapunov exponents of a dynamical system from observed time series," *Phys.Rev.A*, vol. 43, no. 6, pp. 2787-2806, Mar. 1991.

[54] X. S. Yang, "Topological horseshoes in continuous maps," *Chaos Soliton. Fract.*, vol. 33, no. 1, pp. 225-233, Dec. 2005.

[55] F. Yu, L. X. Li, B. Y. He, et al, "Design and FPGA implementation of a pseudorandom number generator based on a four-wing memristive hyperchaotic system and Bernoulli map," *IEEE Access*, vol. 7, pp. 181884-181898, Nov. 2019.

[56] A. Silva-Jurez, E. Tlelo-Cuautle, L. G. Fraga de la, R. Li, "FPAA-based implementation of fractional-order chaotic oscillators using first-order active filter blocks," *Journal of Advanced Research*, vol. 25, pp. 77-85, Sep. 2020.

Kun Tian received bachelor degree in automation from North China university of science and Technology in 2013, and master degree in control theory and control engineering, from Xian University of Technology, in 2016. She is working toward doctoral degree at Xian University of Technology. Her research field is the nonlinear control of complex systems.

Celso Grebogi got his PhD in Physics from the University of Maryland in 1978, Postdoc in Physics and Applied Mathematics at UC Berkeley in 1978-1981. He is the Sixth Century Chair, and the Founding Director of the Institute for Complex Systems and Mathematical Biology, Kings College, University of Aberdeen, UK. He is also an External Scientific Member of the Max-Planck-Society. He was previously with the University of Sao Paulo as Full Professor of Physics, and, before that, with the University of Maryland as Full Professor of Mathematics. He has made a major impact for his work in the field of chaotic and complex dynamics. He was awarded the Senior Humboldt Prize and the Thomson-Reuters Citation Laureate. The seminal work on chaos control (OGY) was selected by the American Physical Society as a milestone in the last 50 years. He received multiple Doctor Honoris Causa degrees, Humboldt Senior Prize, Fulbright Fellowship, Toshiba Chair, and various Honorary Professorship awards. He is Fellow of the Royal Society of Edinburgh, The World Academy of Sciences, Academia Europaea, Brazilian Academy of Sciences, American Physical Society, and the UK Institute of Physics.

Hai-Peng Ren (Member, IEEE) was born in Heilongjiang, China, in March 1975. He received the Ph.D. degree in power electronics and power drives from the Xian University of Technology in 2003. He worked as a Visiting Researcher in the field of nonlinear phenomenon of power converters with Kyushu University, Japan, from April 2004 to October 2004. He worked as a Post Ph.D. Research Fellow in the field of time-delay system with Xian Jiaotong University from December 2005 to December 2008. He worked as an Honorary Visiting Professor in the field of communication with chaos and complex networks with the University of Aberdeen, U.K., from July 2010 to July 2011. From December 2008, he works as a Professor at the Department of Information and Control Engineering, Xian University of Technology, Xian, China. His field includes nonlinear system control, complex networks, and communication with nonlinear dynamics.